MATLYSTATINS, NEW INHIBITORS OF TYPE IV COLLAGENASES FROM *Actinomadura atramentaria*

III. STRUCTURE ELUCIDATION OF MATLYSTATINS A TO F†

HIDEYUKI HARUYAMA, YOSHIKO OHKUMA, HIDEMI NAGAKI, TAKESHI OGITA,††
KAZUHIKO TAMAKI††† and TAKESHI KINOSHITA

Analytical and Metabolic Research Laboratories,
†† Biomedical Research Laboratories, and ††† New Lead Research Laboratories, Sankyo Co., Ltd.,
1-2-58 Hiromachi, Shinagawa-ku, Tokyo 140, Japan

(Received for publication March 7, 1994)

The structures of matlystatins, novel type IV collagenase inhibitors isolated from *Actinomadura atramentaria*, have been determined by a systematic application of homo- and heteronuclear 2D NMR and FAB-MS/MS techniques. Their structures were characterized by the presence of piperazic acid and hydroxamic acid moieties, structural motifs often seen in protease inhibitors.

Among matrix metalloproteinases involved in such biological processes as angiogenesis, rheumatoid arthritis and tumor invasion, the importance of type IV collagenases is well understood in the regulation of degradation process of the basement membranes, of which a major component is type IV collagen.[1] It is known that the activity of type IV collagenases is determined by the balance between the amounts of activated enzymes and the intrinsic inhibitory proteins TIMPs, but an understanding of the effects of recombinant TIMPs on the inhibition of tumor invasion and rheumatoid arthritis has been limited so far,[2,3] partly because of TIMPs' high molecular weights. Thus, the exploration of low molecular weight inhibitors in fermentation extracts of microorganisms has been a promising alternative avenue.

As a result of our efforts in this direction, matlystatins, novel inhibitors of type IV collagenases, were isolated from *Actinomadura atramentaria*.[4,5] In this report, the structure elucidation of matlystatins by application of 2D NMR spectroscopy and FAB-MS/MS spectrometry is described.

Fig. 1. Structures of matlystatins.

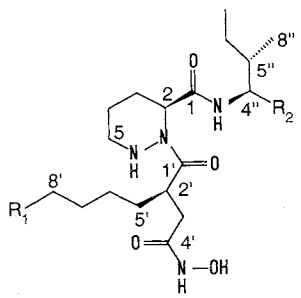

	R_1	R_2
A (**2a**)	CH_3	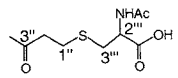
B (**1**)	CH_3	
D (**3a**)	CH_3	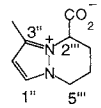
E (**3b**)	H	
F (**3c**)	CH_3	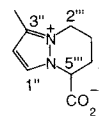

† For part I see ref 4.

Results and Discussion

Physico-chemical properties of the compounds described in this paper have been given in ref 4, unless otherwise stated.

Matlystatin B (1)

In accord with the molecular formula of $C_{22}H_{40}O_5N_4$ established by MS spectral analysis, twenty-two carbon signals were identified in the complete decoupled ^{13}C NMR spectrum of **1**. Since the carbon signals were classified into $4 \times CH_3$, $10 \times CH_2$, $4 \times CH$ and $4 \times C=O$ carbons by DEPT spectra, the sum of non-labile

Fig. 2. Summary of partial structures and their relations in the course of structure elucidation.

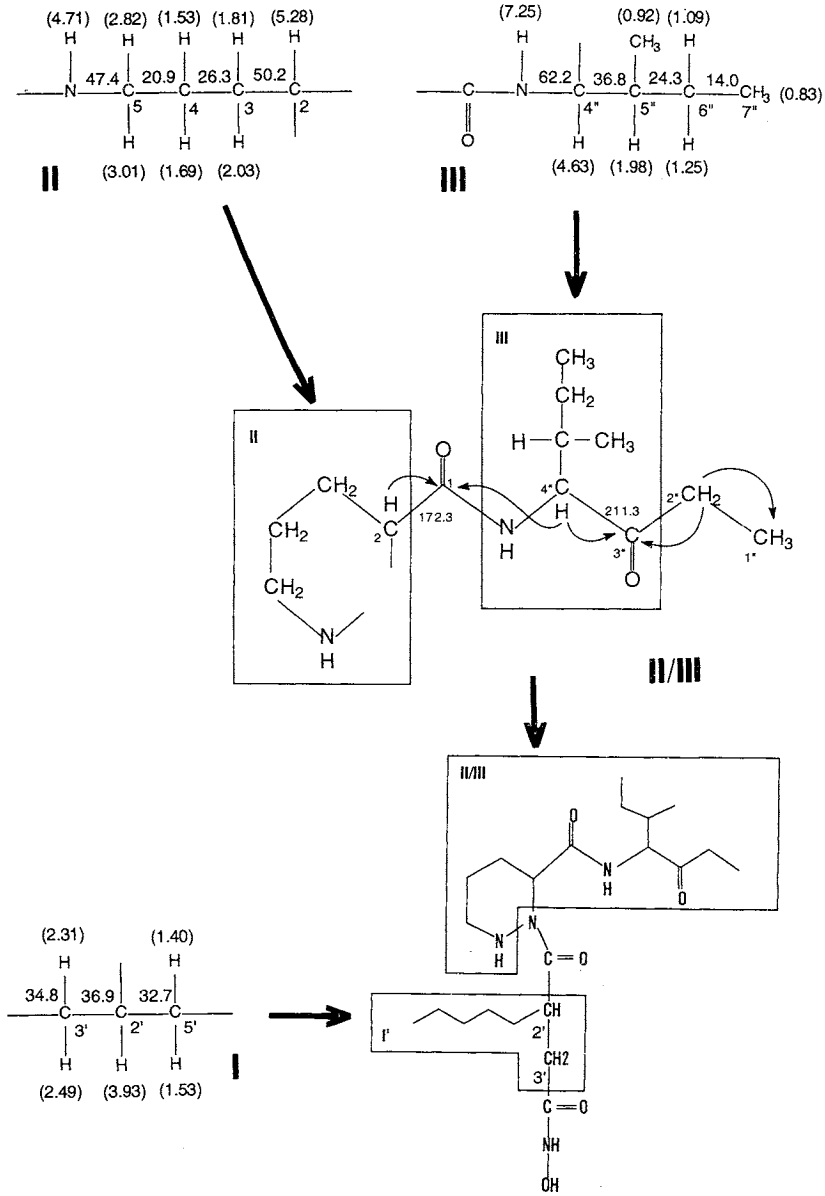

Arrows point ^1H to ^{13}C, between which ^1H-^{13}C long range couplings were observed.

protons amounted to thirty six, indicating the presence of four labile protons. Among these, two were observed at 4.71 and 7.25 ppm. After correlation among carbon signals and proton signals directly bonded to them was established by hetero COSY spectrum, the ^{1}H-^{1}H connectivities were traced on the DQF-COSY spectrum to afford the partial structures **I** to **III** shown in Fig. 2. These partial structures were supported by the relay connectivities derived from HOHAHA spectrum. The labile proton at 4.71 ppm which was coupled to 5-H in the partial structure **II** was assigned to an imino proton, to account for the ^{1}H and ^{13}C chemical shifts of C-5. In the same manner, the labile proton at 7.25 ppm was assigned to an amide proton adjacent to C-4″ in partial structure **III**.

Fig. 3. MS/MS fragmentation pattern of $(M+H)^+$ ions (m/z 441) in FAB-MS spectrum of **1**.

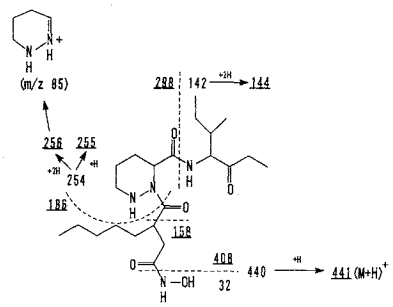

Assembly of these partial structures was carried out by ^{1}H-^{13}C long range correlations derived from the HMBC spectrum, and analysis of the mass fragmentation pattern. Partial structures **II** and **III** could be connected *via* carbonyl carbon C-1 at 172.3 ppm, which exhibited long range couplings to both 4″-H in **III** and 2-H in **II**. To this assembled structure was added an ethyl group, long range-coupled with carbonyl carbon C-3″ at 211.3 ppm, which in turn showed long range correlation to 4″-H. Thus the extended partial structure **II**/**III** was generated as shown in Fig. 2. Partial structure **I** could be extended to partial structure **I′** by combining the *n*-butyl group consisting of a methyl signal at 0.86 ppm and methylene signals around 1.2 ppm, correlations of which were partly established by the ^{1}H-^{13}C long range couplings. ^{13}C chemical shifts through C-5′ to C-9′ could be qualitatively reproduced according to the LINDEMAN-ADAMS rule[6] by assuming C-2′ and C-3′ to be substituted with methyl groups (data not shown).

The FAB mass spectrum of **1** using a glycerol matrix instead of 3-nitrobenzyl alcohol gave a new ion peak at m/z 425 which corresponding to the $(M+H-O)^+$ ion. Such a reduction product ion under the FAB measurement using a glycerol matrix strongly supported the idea that **1** had an *N*-hydroxy group.[7] This constrained the possible functional groups involved in unknown parts to two amide groups, since two nitrogen and three oxygen atoms were left with carbons at 177.3 and 169.8 ppm. First, one nitrogen with no directly bonded proton should be adjacent to C-2 to account for its ^{1}H and ^{13}C chemical shifts and ^{1}H homonuclear coupling pattern. Thus, a hydroxamic acid moiety formed by assembling two unused labile protons with another amide group should be located at the end of the molecule. Finally, the partial structures **II**/**III** and **I′** were connected as shown in Fig. 2 *via* an amide moiety. The formation of piperazic acid (PA) was required to satisfy the unsaturation number of five. A hydroxamic acid moiety might be attached to the partial structure **I′** in the alternative manner. This possibility, however, could be ruled out by the ^{1}H-^{13}C long range couplings observed in matlystatin A.

The major fragmentation pattern of the MS/MS (CAD; collisionally activated dissociation) spectrum of $(M+H)^+$ ion at m/z 441 in the FAB mass spectrum of **1** was consistent with the derived structure as shown in Fig. 3. The compositions of the ions at m/z 441, 408, 298, 144 and 85 in the FAB mass spectrum of **1** using a 3-nitrobenzyl alcohol matrix were determined to be $C_{22}H_{41}O_5N_4$ (obsd. m/z 441.3082; calcd. m/z 441.3078), $C_{22}H_{38}O_4N_3$ (obsd. m/z 408.2871; calcd. m/z 408.2863), $C_{14}H_{24}O_4N_3$ (obsd. m/z 298.1734; calcd. m/z 298.1767), $C_8H_{18}ON$ (obsd. m/z 144.1404; calcd. m/z 144.1388) and $C_4H_9N_2$ (obsd. m/z 85.0782;

calcd. *m/z* 85.0766) by high resolution measurements, respectively. The ^{1}H and ^{13}C NMR data for **1** are listed in Tables 1 and 2.

Matlystatin A (**2a**) and its Amide Derivative (**2b**)

The molecular formula of matlystatin A, $C_{27}H_{47}O_8N_5S$, was established by mass spectral analysis, while a closely related compound with molecular formula $C_{27}H_{47}O_7N_5S$ was isolated as a by-product,[4] of which physico-chemical data are given in the experimental section. The close similarity of the ^{1}H and ^{13}C NMR spectra for **2a** and **2b** suggested that the structural difference between them occurred in a quite limited part of the molecule. Analysis of mass fragmentation described below disclosed that the hydroxamic acid group in **2a** was replaced with an amide group in **2b**. In spite of the close structural similarity, the stabilities of **2a** and **2b** were different. As matlystatin A was easily decomposed in methanol-d_4 in one day, the spectral analysis of **2b** was first carried out.

The strategy for structure elucidation was the same as described in the previous section. Following the identification of CH_3, CH_2, CH and quaternary carbons by DEPT spectra, directly bonded protons were assigned by a hetero-COSY spectrum. Tracing of DQF-COSY and HOHAHA spectra disclosed the proton spin systems corresponding to pentyl succinic acid (PSA), and PA moieties seen in **1**. In addition, the spin system of the partial structure **II** (Fig. 2) and another isolated spin systems of $-CH_2-CH-$ and $-CH_2-CH_2-$ were identified.

Based on the ^{1}H-^{13}C long range couplings summarized in Fig. 4, the spin system of $-CH_2-CH-$ could be extended to the partial structure **IV** by adding the *N*-acetyl and carbonyl groups, while the spin system of $-CH_2-CH_2-$ could be combined with partial structure **III** to afford 4-amino-5-methyl-3-heptanone (AMH) moiety, another common structural element seen in matlystatin A and B. The connection of AMH and PA units was confirmed by long range coupling of the carbonyl carbon at 174.3 ppm to 4″-H and NH in AMH and 2-H in PA. The long range coupling between the terminal amide proton at 6.67 ppm and C-3′ fixed a way to

Fig. 4. The summary of ^{1}H-^{13}C long range couplings to connect the structural units in **2b**.

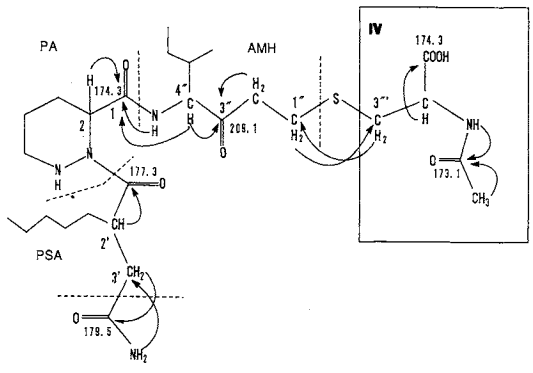

The arrows point ^{1}H to ^{13}C.

Fig. 5. MS/MS fragmentation patterns of $(M+H)^+$ and $(M-H)^-$ ions (*m/z* 586 and *m/z* 584, respectively) in the FAB-MS spectra of **2b**.

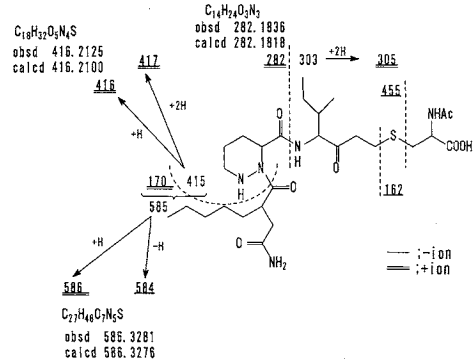

Fig. 6. MS/MS fragmentation patterns of $(M+H)^+$ and $(M-H)^-$ ions (*m/z* 602 and *m/z* 600, respectively) in the FAB-MS spectra of **2a**.

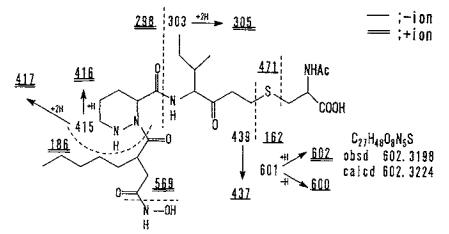

incorporate the PSA unit into the molecule, as shown in Fig. 4.

Thus partial structure **IV** should be attached to the AMH end as evidenced by the ^{1}H-^{13}C long range couplings between 3‴-H and C-1″, and between 1″-H and C-3‴ (see Fig. 4). The location of the sulfur atom between the AMH and partial structure **IV** was expected by elimination, and explicitly evidenced by the mass fragmentation pattern shown in Fig. 5.

Once the structure of **2b** had been established, the structure of **2a** was automatically derived. As mentioned in the section on matlystatin B (**1**), a new ion peak at *m/z* 586 corresponding to $(M+H-O)^+$ ion appeared in the FAB mass spectrum of **2a** using a glycerol matrix, whereas such a reduction product ion was not detected in **2b**. The fact that MS/MS spectrum of $(M+H-O)^+$ ion from **2a** coincided with that of $(M+H)^+$ ion of **2b** was consistent with the reduction of –NHOH moiety to $-NH_2$ in **2b**. The mass fragmentation pattern for **2a** is shown in Fig. 6. The ^{1}H and ^{13}C NMR data for **2a** and **2b** are listed in Tables 1 and 2.

Matlystatins D (**3a**), E (**3b**), and F (**3c**)

The molecular formulae of **3a**, **3b** and **3c** were established from detection of the $(M+H)^+$ ions using high resolution FAB mass spectrometry (see, Fig. 7). The molecular formula of $C_{27}H_{44}N_6O_6$ for both **3a** and **3c** suggested that matlystatin F is an isomer of matlystatin D. On the other hand, the molecular formula of **3b** of $C_{26}H_{42}N_6O_6$ indicated that one CH_2 unit was missing compared with **3a** and **3c**.

The major fragment ions obtained from FAB-MS/MS spectra of $(M+H)^+$ ions are summarized in Fig. 7. Analysis of the mass fragmentation pattern disclosed that the common part consisting of PA, PSA, and the terminal hydroxamic acid unit was conserved in both **3a** and **3c** as other matlystatins discussed so far, while the difference between **3a** and **3b** was detected at the substituted succinic acid part, where the pentyl succinic acid commonly found in other matlystatins was replaced with butyl succinic acid.

Analysis of ^{1}H and ^{13}C NMR spectra for **3a** confirmed retention of the common structural units, and at the same time exhibited the presence of the other structural units shown in Fig. 8. The ethyl ketone part of the AMH moiety was replaced with the =C(X)–CH=CH– unit to form the partial structure **V**. The partial structure **V** attached to PA moiety at its NH end as evidenced by the ^{1}H-^{13}C long range couplings of C-1 to 4″-H and NH at 8.54 ppm. Another structural unit **VI** was derived from the ^{1}H-^{1}H connectivities from DQF-COSY and HOHAHA spectra.

Since no proton except those involved in the partial structures **V** and **VI** were left as elements to form

Fig. 7. Major fragment ions obtained from FAB-MS/MS spectra of $(M+H)^+$ ions of **3a**, **3b** and **3c**.

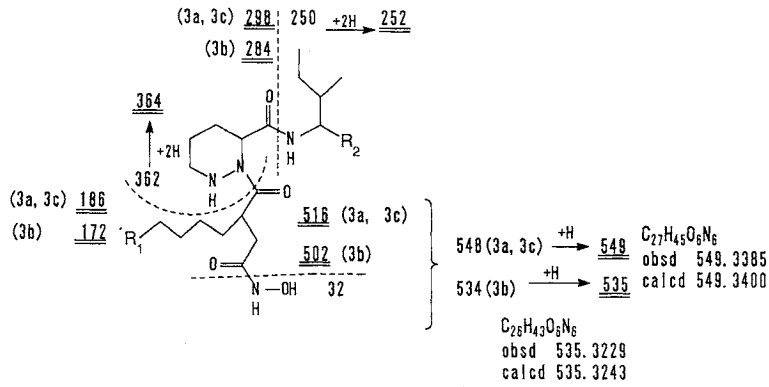

R_1 and R_2 correspond to those in Fig. 1.

Fig. 8. The partial structures **V** and **VI** with NMR data.

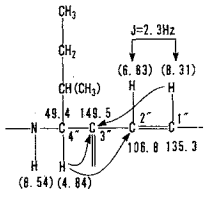

Partial structure **V**

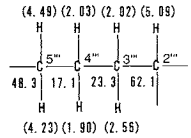

Partial structure **VI**

The ^{1}H chemical shifts are in the parentheses. The arrows point ^{1}H to ^{13}C between which long range couplings were observed, while double headed arrow indicates ^{1}H-^{1}H coupling.

Fig. 9. The ROEs specific to the fused ring geometries in **3a**, **3b** and **3c**.

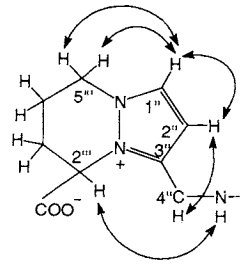

3a and **3b**

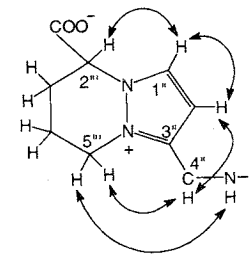

3c

Table 1. ^{1}H NMR chemical shifts data for matlystatins and an amide derivative.

	1 ($CDCl_3$)	**2a** (CD_3OD)	**2b** (CD_3OD)	**3a** (DMSO-d_6)	**3c** (DMSO-d_6)
2-H	5.28	5.17	5.18	4.97	5.00
3-H	1.81, 2.03	1.98, *ca.* 2.1	1.96, 2.13	1.68, 1.97	1.71, 1.90
4-H	1.53, 1.69	1.54, 1.70	1.52, 1.69	1.30, 1.48	1.34, 1.38
5-H	2.82, 3.01	2.87, 3.05	2.86, 3.00	2.63, 2.87	2.65, 2.87
NH	4.71	—	4.87[a]	—	4.74
2'-H	3.93	3.98	3.92	3.63	3.69
3'-H	2.31, 2.49	2.20, 2.40	2.29, 2.53	1.99, 2.25	1.96, 2.23
5'-H	1.40, 1.53	1.41, 1.56	1.40, 1.55	1.34, 1.44	1.37, 1.37
6'-H	1.24	1.28	1.30	1.18	1.12
7'-H	1.20	1.26	1.25	1.26	1.16
8'-H	1.24	1.30	1.30	1.34	1.20
9'-H	0.86	0.88	0.88	0.84	0.86
NH	—	—	6.67[a], 7.17[a]	10.31	—
1''-H	1.09	2.80	2.78	8.31	8.30
2''-H	2.55	2.86	2.84	6.83	6.75
4''-H	4.63	4.40	4.39	4.84	4.80
5''-H	1.98	1.98	1.96	1.94	1.88
6''-H	1.09, 1.25	1.19, 1.40	1.19, 1.40	1.17, 1.49	1.15, 1.58
7''-H	0.83	0.89	0.90	0.82	0.86
8''-H	0.92	0.94	0.93	0.76	0.78
NH	7.25	—	8.24[a]	8.54	8.80
2'''-H	—	4.59	4.57	5.09	4.96
3'''-H	—	2.88, 3.04	2.86, 3.03	2.02, 2.56	2.16, 2.46
4'''-H	—	—	—	1.90, 2.03	1.97, 1.97
5'''-H	—	—	—	4.23, 4.49	4.12, 4.61
1'''-Me	—	2.02	2.01	—	—

[a] Chemical shifts read in DMSO-d_6.

unknown part of **3a**, a carboxylic acid group, of which presence was suggested from mass fragmentation analysis, must exist as a carboxylate anion. Accordingly, the anti-symmetric, $-COO^-$ streching band characteristic for carboxylate anion was observed around 1544 cm^{-1} in the IR spectra of **3a**, **3b** and **3c**, but absent in other matlystatins.[4] The small vicinal coupling constant between 1''-H and 2''-H (J=2.3 Hz) was consistent with the other strained five-membered ring systems reported so far.[8]

The ROEs observed between 1''-H and 5'''-H and between NH and 2'''-H determined the way to assemble partial structures **V** and **VI** as shown in Fig. 9. The immonium cation on the nitrogen was required to compensate for the carboxylate anion. Thus, the structure of **3a** was established as shown in

Table 2. ^{13}C chemical shifts data for matlystatins and related compounds.

	1 ($CDCl_3$)	**2a** (CD_3OD)	**2b** (CD_3OD)	**3a** (DMSO-d_6)	**3c** (DMSO-d_6)
C-1	172.3	174.6	174.3	170.9	171.9
C-2	50.2	52.1	51.9	50.1	49.7
C-3	26.3	27.4	27.6	25.7	25.9
C-4	20.9	22.0	22.2	20.6	20.7
C-5	47.4	47.9	47.9	46.5	46.3
C-1′	177.3	179.6[a]	177.3	175.6	175.9
C-2′	36.9	37.9	38.0	36.7	35.6
C-3′	34.8	36.2	38.7	34.6	34.6
C-4′	169.8	171.8[a]	179.5	167.9	167.9
C-5′	32.7	33.7	33.7	31.6	31.7
C-6′	26.3	27.3	27.5	25.7	25.7
C-7′	31.8	32.9	33.0	31.3	31.3
C-8′	22.4	23.4	23.5	21.8	21.8
C-9′	14.0	14.4	14.4	13.8	13.8
C-1″	7.6	27.0	26.9	135.3	138.4
C-2″	34.6	42.0	42.0	106.8	104.5
C-3″	211.3	209.8	209.1	149.5	149.8
C-4″	62.2	64.2	64.2	49.4	48.6
C-5″	36.8	36.9	36.9	36.7	37.2
C-6″	24.3	25.7	25.7	24.5	24.5
C-7″	11.5	11.7	11.7	10.4	10.5
C-8″	16.1	16.4	16.4	15.5	14.8
C-1‴	—	173.1	173.1	166.4	167.5
C-2‴	—	54.0	54.0	62.1	64.0
C-3‴	—	35.1	35.2	23.3	23.0
C-4‴	—	—	—	17.1	17.4
C-5‴	—	—	—	48.3	46.9
Me-1‴	—	22.6	22.6	—	—
COOH-2‴	—	174.6	174.3	—	—

[a] The assignments may be exchangeable.

Fig. 1. Since similar ROEs were observed in **3b**, its structure could be established.

Comparison of the mass fragmentation patterns of **3a** and **3c** revealed no major differences except in the intensities of some fragment ions. An identical set of partial structures was identified from analysis of the ^1H and ^{13}C NMR spectra. Therefore, the structural difference between **3a** and **3c** seemed to be at the junction of the five and six membered ring systems. The ROEs observed between 1″-H and 2‴-H and between 4″-H and 5‴-H led to the alternative way of ring fusion in **3c**, in which 2‴-H stands close to 1″-H (see, Fig. 9).

The ^1H and ^{13}C NMR data for **3a**, **3b** and **3c** are summarized in Tables 1 and 2. The authors are not aware of the reported ring system identical to those in **3a**, **3b** and **3c**. However nigellicine may be an example of the related ring system, in that nigellicine is a natural product possessing N–N bond and an intramolecular carboxylate anion-immonium cation pair.[9]

Stereochemistry of Matlystatins

The stereochemistry of the C-2′ position of matlystatins was determined by degradation study. Acid hydrolysis of matlystatin A by refluxing with Dowex 50W (H^+) for four hours followed by ether extraction gave 2-pentyl succinic acid. Since its specific rotation value of $-15.4°$ coincided with that of a known sample of *R* enantiomer,[10] the absolute configuration of C-2′ was determined as *R*. An attempt to isolate piperazic acid in acid hydrolysate failed. The absolute configurations of the other chiral centers at C-2,

C-4″ and C-5″ were established by synthetic studies described in the accompanying paper.[11]

Experimental

General

Matlystatins were prepared as described in the previous papers.[4,5] ^{1}H and ^{13}C NMR spectra were measured with a JEOL GX-400 NMR spectrometer and processed on SUN4/110 workstation using NMR1/2 software. Chemical shifts are expressed in ppm with TMS as internal standard.

FAB mass spectra and FAB-MS/MS (CAD) spectra were obtained with a JEOL JMS-SX/SX102A tandem mass spectrometer (BEBE geometry) using a 3-nitrobenzyl alcohol matrix unless otherwise noted in the text. Xenon was employed as source of the first atom beam (6 KeV), and the mass spectrometer was operated at an accelerating voltage of 10 kV. To obtain MS/MS (CAD) spectra, argon was used as the collision gas and was introduced into a collision cell in the third field-free region, to give an approximate 80% reduction of the intensity of the selected precursor beam.

An Amide Derivative of Matlystatin A (**2b**)

2b was separated from crude matlystatin A in the final step of purification by HPLC described in ref 4. **2b** is a white hygroscopic powder, mp 69~72°C, $[\alpha]_D$ −40.5° (*c* 0.2, MeOH). An ultraviolet spectrum acquired in methanol contains no band except end absorption. An infrared spectrum acquired as KBr pellet contains bands at: 3308, 1718, 1664 and 1627 cm^{-1}.

References

1) STETLER-STEVENSON, W. G.; Type IV collagenases in tumor invasion and metastasis. Cancer and Metastasis Reviews 9: 289~303, 1990
2) DECLERK, Y. A.; T.-D. YEAN, D. CHAN, H. SHIMADA & K. E. LANGLEY: Inhibition of tumor invasion of smooth muscle cell layers by recombinant human metalloproteinase inhibitor. Cancer Res. 51: 2151~2157, 1991
3) ALBINI, A.; A. MELCHIORI, L. SANTI, L. A. LIOTTA, P. D. BROWN & W. G. STETLER-STEVENSON: Tumor cell invasion inhibited by TIMP-2. J. Natl. Cancer Inst. 83: 775~779, 1991
4) OGITA, T.; A. SATO, R. ENOKITA, K. SUZUKI, M. ISHII, T. NEGISHI, T. OKAZAKI, K. TAMAKI & K. TANZAWA: Matlystatins, new inhibitors of type IV collagenases from *Actinomadura atramentaria*. I. Taxonomy, fermentation, isolation and physico-chemical properties of matlystatin group compounds. J. Antibiotics 45: 1723~1732 1992
5) TANZAWA, K.; M. ISHII, T. OGITA & K. SHIMADA: Matlystatins, new inhibitors of type IV collagenases from *Actinomadura atramentaria*. II. Biological activities. J. Antibiotics 45 : 1733~1737, 1992
6) LINDEMAN, L. P. & J. Q. ADAMS: Carbon-13 Nuclear Magnetic Resonance Spectrometry, Chemical Shifts for the Paraffins through C9. Anal. Chem. 43: 1245~1252, 1971
7) NAKAMURA, T.; H. NAGAKI & T. KINOSHITA: Reduction of aryl halides and N-hydroxy nitrogen compounds in fast atom bomberdment mass spectrometry. Bull. Chem. Soc. Jpn. 58: 2798~2800, 1985
8) BATTERHAM, T. J.: NMR Spectra of Simple Heterocycles. pp. 250~303, John Wiley & Sons, New York, 1973
9) RAHMAN, A.-UR; S. MALIK, H. CUN-HENG & J. CLARDY: Isolation and structure determination of nigellicine, a novel alkaloid from the seeds of *Nigella sativa*. Tetrahedron Lett. 26: 2759~2762, 1985
10) GORDON, J. J.; J. P. DEVLIN, A. J. EAST, W. D. OLLIS, I. O. SUTHERLAND, D. E. WRIGHT & L. NIET: Studies concerning the antibiotic action. Part I. The constitution of actinonin. A natural hydroxamic acid with antibiotic activity. J. Chem. Soc. Perkin I. 1975: 818~825, 1975
11) TAMAKI, K.; S. KURIHARA, T. OIKAWA, K. TANZAWA & Y. SUGIMURA: Matlystatins, New Inhibitors of Type IV Collagenases from *Actinomadura atramentaria*. IV. Synthesis and structure - activity relationships of matlystatin B and its stereosiomers. J. Antibiotics. 47: 1481~1492, 1994